Modelling Graphene-based Transparent Electrodes for Si Solar Cells by Artificial Neural Networks

[1]Z.Meziani and [2]Z.Dibi

[1-2]Advanced Electronic Laboratory (LEA), Faculty of Technology, Department of Electronic, University of Batna2, Algeria

E-mail:[1]meziani_zahra@hotmail.fr

ABSTRACT

Transparent electrodes based on conductive transparent oxides (TCO) are increasingly invading the photovoltaic (PV) field because of their unique ability to reconcile high transparency with good electrical conductivity. The TCO market is dominated by the Indium oxide doped with Tin (ITO) with a resistivity of 30-80 Ω/sq and a transmittance of 90 % in the visible range. Yet, its cost is rising due to the high indium content, is one of the reason that encouraging research on alternative materials essential for the development of PV technologies. It is in this theme that graphene, a material with exceptional properties, is tested as a design material for transparent electrodes for Si solar cells. In this paper, we optimized optically and electronically the graphene-based transparent electrodes (G-TE) by proposing a model of simulation based on artificial intelligence and specifically artificial neural networks (ANN) which is the ANN-model. Therefore, to achieve an appropriate characterisation of a behaviour of G-TE for the Si solar cells, the ANN-model has been performed to simulate and optimise different parameters of the G-TE, by controlling graphene layer number, tuning graphene work function, and deduce the suitable transmittance and resistivity in order to have a complete adjustment for these parameters. Our study mentioned that a G-TE with three layers of graphene and a work function of 4.75 eV leads for a sheet resistance of 50 Ω/sq and transmittance of 91.4 %; these results suggest that G-TE is a promising candidate in the TCO field.

Keywords: *Graphene, transparent electrodes, Indium Tin oxide, Si solar cells, artificial neural networks (ANN), ANN-model.*

1. INTRODUCTION

The cost of photovoltaic technology is mainly related to the cost of the materials used and the cost of the manufacturing process. One of the most expensive materials is that used for the fabrication of the transparent electrode. A material commonly used as a transparent electrode in PV devices is ITO, which has excellent electrical and optical properties and can be produced on a large scale [1]. However, the large scarcity of indium reserves and a significant increase in demand has led to an increase in the price of indium [2]. Therefore, exploration of new materials for transparent electrode applications is necessary to achieve low cost and high efficiency. Potential replacement materials include metal grids [3-4], metal oxides [5-6], and thin film metals [7-8]. Low sheet resistivity and high optical transmittance are the fundamental requirements for these electrodes. Currently, neither ITO nor the alternative electrodes satisfy the industry's future requirements.

Graphene, a two-dimensional material made up of a monolayer of carbon atoms oriented in a hexagonal network, has attracted a great deal of scientific attention since its discovery in 2004 by K.S. Novoselov and A.K.Geim [9]. This is due to its exceptional properties, such as electronic mobility greater than 200 000 cm². V-1.s-1 [9] and mechanical properties by making a flexible and extremely resistant material [10]. Moreover, the high transparency of a graphene monolayer, 97.7% [11], makes it possible to envisage it as transparent electrodes for solar cells.

Experimental studies have been performed to optimize the characteristic of the sheet of graphene used as solar cells transparent electrodes, for that several parameters are studied : layer number of graphene, resistivity, transmittance, doping status …; the stake is to find the adequate recombination of this parameters which gives us better results.

In this paper, a theoretical model is presented to simulate the performance of G-TE for solar cells using artificial intelligence interpreted by the ANN-model. Using parameters extracted from experiments, our simulation gives consistent results with tested performance. Based on our theoretical analysis, two practical optimization treatments have been proposed : the work function (*WF*) and layer number (*N*) of graphene should be carefully adjusted and thereafter deduce the transmittance (*T*) and sheet resistance (*Rsh*) of our G-TE.

2. GRAPHENE AND ITS APPLICATION AS TRANSPARENT ELECTRODES IN PV

2.1. Graphene Physics

Graphene is defined as a single layer of carbon atoms arranged in a hexagonal lattice. Its atomic structure can also be used as a basic building block to construct other carbon-based materials: it can be folded into fullerenes, rolled up into nanotubes, or stacked into graphite. The carbon allotropes (Fig. 1a), from zero-dimensional (0D) fullerenes, one-dimensional (1D) carbon nanotubes (CNT), to three dimensional (3D) graphite and diamond are all bonded by various combinations of the four $2s^2 2p^2$ orbital valence electrons of each carbon atom.
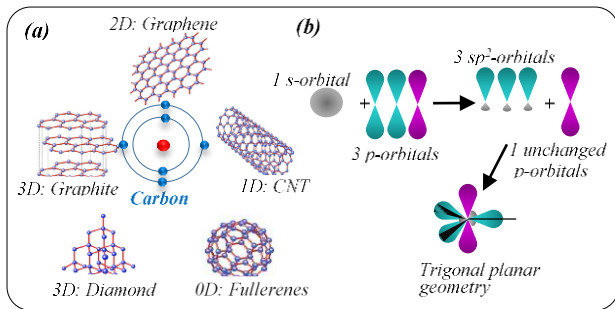
Fig. 1. (a) Schematic of carbon atom and carbon allotropes, from 0D to 3D; (b) atomic orbitals of graphene

In 2D graphene, a carbon atom shares electrons with three nearest neighbours (Fig. 1b), in the form of three sp^2 bonds, leaving out-of-plane p_z orbitals with one electron per atom. The three electrons forming the sp^2 bonds are responsible for the outstanding mechanical and thermal properties of graphene. On the other hand, the electrons in the p_z orbitals can easily hop between the neighbouring atoms, since the hopping energy is high (~ 3.0 eV), and thus form the π bands in the conduction bands (Ec) and π^* bands in the valence bands (Ev). These electrons contribute to the outstanding electrical properties of graphene. As shown in Fig. 2c, E_C and E_V meet at the six corners of the first Brillouin zone (named as Dirac points) resulting in a zero bandgap. Hence, graphene behaves like a semi-metal [9].
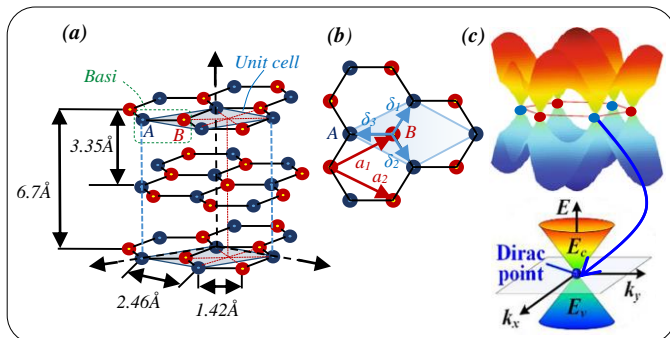

Fig. 2. (a) schematic representation of graphite formed with staking graphene and bond length; (b) unit cell, basis of graphene ; (c) energy dispersion of graphene, where the energy dispersion is linear for low energies near the six corners (Dirac points) of the two-dimensional hexagonal Brillouin zone.

2.2. GraphenePreparation and Transfer

Graphene can be fabricated mainly by two techniques:

Physical technique-which involves:

- Micromechanical exfoliation of highly ordered pyrolytic graphite (HOPG) [9], with this technique we obtain samples of high crystalline quality but their dimensions are inadequate to use as a transparent electrodes (samples in order of micrometer).

- Sublimation of silicon from SiC at high temperatures [12-13], but the high cost of SiC substrates is the major inconvenient to use this method for producing G-TE.

Chemical technique-which involves:

- Reduction of graphene oxide [9-14], the electrical

properties of these films are lower.

- Chemical vapor deposition (CVD) on metal catalyst substrates [15].

The CVD method produce large- scale and high quality of graphene. In this method, usually, Cu foil [16] or Ni layers [15-17] are used as the catalyst, and CH_4 is used as the carbon source with H_2 as the carrier gas. The synthesized graphene is usually transferred to the device substrate with the help of PMMA [poly (methyl methacrylate)]. It is reported that graphene synthesized by CVD electrically and optically outperforms ITO [18] and thus is promising in serving as a transparent conductivefilm [17-16-15-1].

With the growth of graphene on copper, we obtain samples of more than 95% monolayer graphene [19]. The use of monolayer graphene makes it possible to have a better control over the transparency of the electrodes produced by stacking several layers of graphene.

Despite the exceptional mechanical properties of graphene [10], its thickness of a few atomic layers makes it very difficult to transfer its samples (on the order of centimetre) without causing rupture to the graphene. For this reason, most graphene transfers are carried out by adding a mechanical support, and the most frequently used material is a polymer, the PMMA (poly (methyl methacrylate)), chosen by Reina et al. [15] and by Li et al. [16]. The PMMA layer is sufficiently resistant mechanically while remaining flexible, which ensures good conformity between the graphene and the substrate.

For the step of metal sheet dissolution, different chemical solutions are used. A solution of $FeCl_3$ [17-20] or HCl [15] used for nickel sheet, and a solution of Fe $(NO_3)_3$ [16-21-22-23-24] used for copper sheet.

When the metal sheet is completely dissolved, the graphene film floating on the surface of the solution is then rinsed in deionized water and recovered directly on the desired substrate. The samples are then dried. It is then possible to remove the mechanical support (PMMA), by immersing the samples in acetone [15-16-21-23-25]. Figure 3 summarise the essential steps for transfer process of graphene.
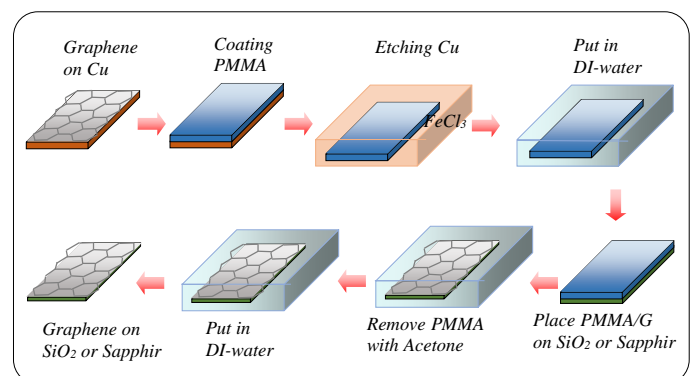

Fig. 3. Transfer process of graphene

2.3 Graphene/Semiconductor Schottky Junction

Because of the near-zero band-gap and high conductivity characteristics of graphene, the graphene/n-type semiconductor heterojunction can be taken as a metal/semiconductor Schottky junction (assuming the work function difference between the graphene and the semiconductor is large enough) [26-21-27]. Recently, several studies [28-29-30-31-32] proposed a photovoltaic model in which highly conductive, transparent graphene films is coated on n-type silicon (n-Si) wafer to form Schottky junction [33]. The results of these studies showed that in this Schottky solar cell, graphene as energy conversion materials not only contributes to charge separation and transport, but also functions as transparent electrode.
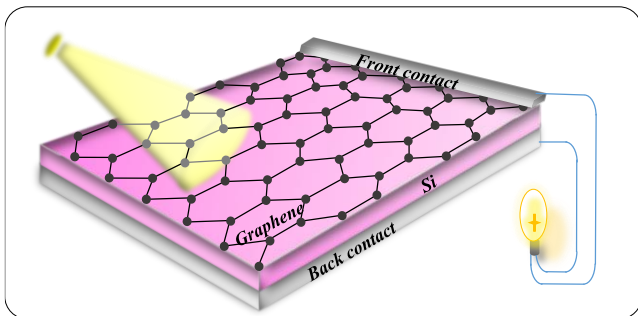

Fig. 4. A graphene/semiconductor photovoltaic device

The mechanism of such Schottky junction solar cell can be understood qualitatively by plotting the energy band diagram. Figure 6.a shows the energy diagram of a graphene/ n-type semiconductor Schottky junction solar cell under illumination. Due to the work function difference between the graphene (ϕ_G), and semiconductor (ϕ_S), a built-in potential forms in the semiconductor near the interface. Under light illumination above the bandgap, the photogenerated holes and electrons are separated and driven towards the Schottky electrode (graphene film) and semiconductor layer, respectively, by the built-in electric field. We assume that the junction between graphene and semiconductor is an ideal Schottky contact, so the built-in potential ϕ_{bi} equals the work function (WF) difference of these two materials:

$$\phi_{bi} = \phi_G - \phi_S = \phi_G - \chi - kTln\left(\frac{N_D}{N_C}\right)\ldots\ldots(1)$$

Where χ is the semiconductor electron affinity, as shown in figure 6, N_D and N_C are the doping and the effective electron state concentration of semiconductor, respectively. As graphene is metallic, n-type silicon is chosen as the substrate to obtain a comparatively large built-in potential. If the graphene WF becomes larger, a stronger electric field will be formed on the semiconductor side of the junction, hence improving the junction's capacity to collect photo-generated carriers. The mechanism of tuning the WF of graphene is rather straightforward. As shown in figure 6.b, the dispersion of mobile π electrons in monolayer graphene near the Dirac point in the first Brillouin zone (BZ) is in a linear correlation. For intrinsic graphene, the Fermi energy is located at the crossing point of the π and π* bands, which renders the carrier density at a low level at room temperature. However, if the Fermi energy is shifted away from the original position (figure 6.c), more electrons or holes can be activated to participate in the conduction process. Therefore, graphene with shifted Fermi energy (i.e., modulated WF) performs better in conducting.

The WF of graphene can be tuned either by an applied electric field or by proper chemical doping, as summarized in figure 5. For example, AuCl₃ doping can improve the WF to as high as 5.1 eV. Devices are fabricated with various chemical treatments and measured their series resistances and built-in potential changes, which are plotted as a function of the chemical treatment time. The series resistance decreases and the built-in potential increases at longer chemical treatment time. These changes reflect the modified WF.
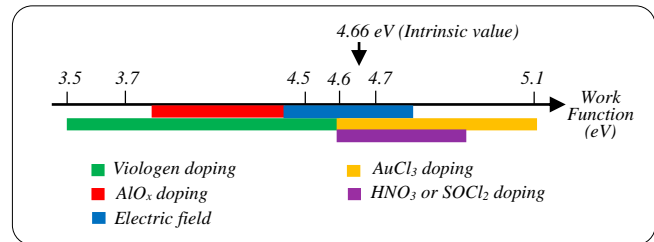

Fig. 5. WF modulation of graphene, including electric field effect [34] and chemical doping with Viologen [35], AlOx [36], HNO₃ [27], SOCl₂ [27] and AuCl₃ [27].

After chemical doping, the transmittance T is almost unchangeable, furthermore, the sheet resistance R_{sh} has rapidly decreased after chemical doping [32], and a several analysis of the dependence of R_{sh} on WF[37,32], from which it is known that R_{sh} decreases significantly upon a tiny shift of WF from its intrinsic state.
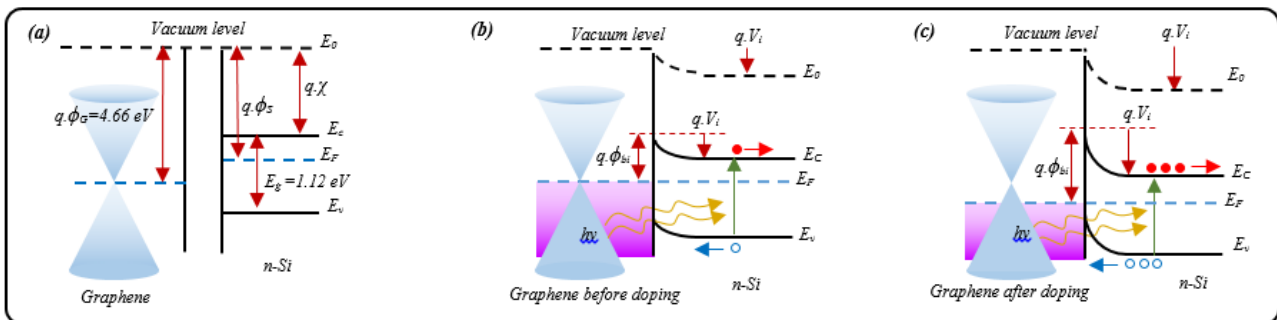

Fig. 6. (a) The energy band diagram of the graphene and n-Si semiconductor, (b) The energy band diagram of the graphene/n-Si Schottky junction before doping graphene, (c) after doping graphene.

3. CHARACTERISATION OF G-TE WITH ANN

The ANN is the adequate technology for the resolution of estimation and prediction problems. ANN's methods are used to expand the range of potential applications in various fields due to the functionality of the black box of the neural network [38-39].

The objective of this work is to create an ANN model who can faithfully reproduce the response of the solar cells G-TE. This theoretical model is presented to simulate the performance of the G-TE. For this, we must determine parameters who have influences on the performance of the G-TE, and thereafter we dispatch up theme into input parameters and output parameters. Figure 7 shows the schematic of the black box of our ANN model.
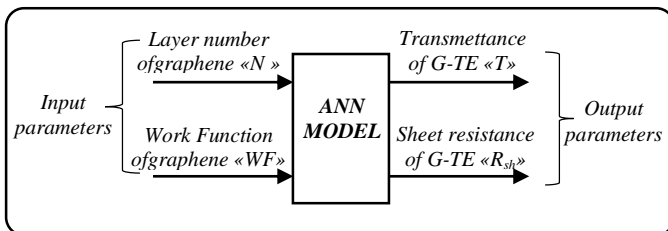

Fig. 7. Input and output parameters of the ANN model

We have to optimise the transmittance and the sheet resistance (hence the conductivity) of our G-TE by control the layer number and the work function of graphene. Figure 8 shows an example for (R_{sh}-T) relationship for samples of ITO-TE and G-TE.

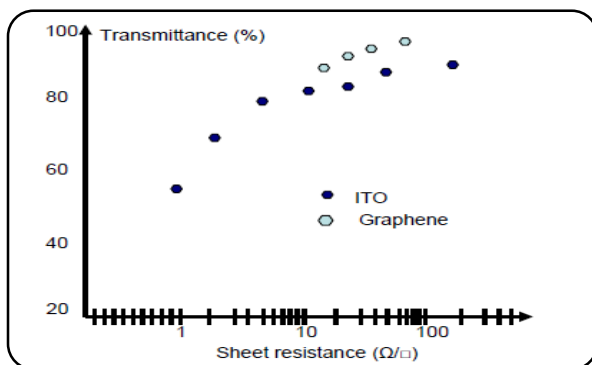Fig. 8. Transmittance vs sheet resistance for state-of-the-art Graphene & ITO (adapted from [40-18-41-42-1]).

3.1. ANN Model Designing

The ANN model of our design process can be summarised in these stages [43-44-45]:

- Collecting a database characterised by the input and output parameters.
- Separation of the database into three subsets (training base, validation base and test base).
- The choice of the architecture of the ANN (Selection of inputs, outputs, number of hidden layers, number of neurons per layer, the activation functions ...).
- Training the neural network on the bases of Training and validation.
- Measurement of neural network performance on the test base.

Our study focuses on the recent research on G-TE and all the graphene involved in this highlights are synthesized by the CVD method on copper foils [46-47-37-29-30-32].

3.2. Collecting the Database

The database includes the ANN inputs and associated outputs, and therefore it determines both network size (and hence the simulation time) and performance. For our training, we have used different curves, associating each value of Layer number (N) and work function (WF) of graphene an R_{sh} or T value of G-TE. Figure 9 shows a sample of curves used in our study adapted from [47]
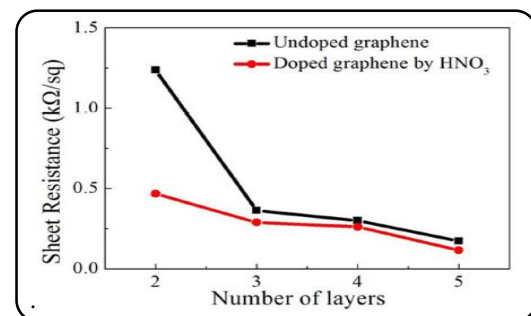

Fig. 9. Sample of curves used in the database [47].

To realize our ANN model the database is composed of 1390 elements divided into 03 sub-base:

- Training base.
- Validation base.
- Test base.

It should be noted here that there are no specific rules concerning this separation, however, in general the training set must include a significant percentage of the given base that can exceed 60%, for validation base it represents between 20% and 30% of the database, and finally the test base is between 10% and 25% of the database, depending on the problem at hand [48]. In our work the training base is composed of 834 elements (60%), the validation base is composed of 417 elements (30%) and the test base is composed of 139 elements (10%). It is important to not use any element of the test base during the training. This database is available only to the final performance measurement. In other words, it is used to check if the neural network has a good performance on the examples that are not learned before (test base).

3.3. Choice of the Architecture of the ANN

We can make a classification for an ANN according to its architecture, training selected and the activation function used. The simplest and most known of ANN and most used for approximation and prediction problems is the multilayer perceptron (MLP) [43]. It consists of several neural layers generally connected in a feed forward structure. The calculation of the output is done by propagating the calculations from left to right, with a supervised training. The activation function used is primarily the sigmoïd function [43-44]. To drive the MLP, the training algorithm used is usually the algorithm of back propagation [43]. According to [49-50-51] an MLP with two hidden layer having a sigmoïdal activation function in the first layer and a linear function in the output layer, allows one to approximate the function studied with acceptable accuracy,

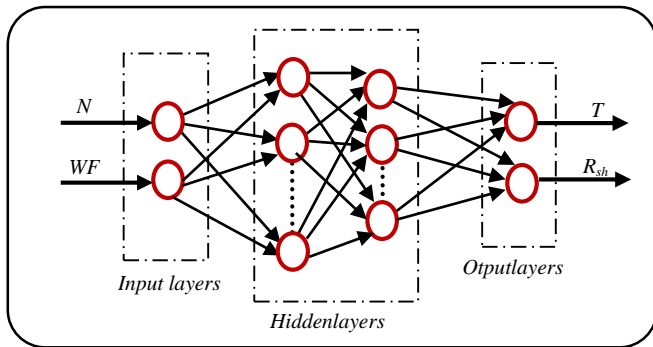provided you have enough neurons on hidden layers (Figure 10).

Fig. 10. Architecture of the MLP used

The structure of our MLP network is mainly determined by experiment, since the number of nodes in the input layer and the output layer is based on the number of input and output parameters, respectively. The case is not easy for the number of neurons in the hidden. In fact, with a limited number of neurons (too small), the network will not be performing on training, and with a number of excessive weight, the network may have poor generalisation properties (phenomenon of over-training).The solution to remedy to this problem is to build multiple architectures and select the most suitable model for our application.We retain the architecture that gives the minimum mean square error (*MSE*).

4. RESULTS AND DISCUSSION

Once all training steps are performed, our MLP is formed and performance measures compared to experimental data is needed to test the reliability of our ANN model, for this we cross to the test phase.

4.1 Test Phase and Measuring the Performance of the ANN Model

In this phase, it is necessary to carry out tests to estimate the quality of the generalisation. Figure 12 shows the performance of the ANN model obtained for the curves used, the solid lines plot the experimental data and the dashed lines present our simulation interpreted by our ANN model. The layer number N is an important parameter that influences both the transmittance T and the sheet resistance R_{sh} of graphene, and thus determines the G-TE performance. Figure 12 (a) and (b) plot the transmittance and the sheet resistance of intrinsic graphene as a function of layer number, respectively, using the experimental values and the theoretical method mentioned previously (ANN model). As the layer number increases, the sheet resistance decreases dramatically, which improves the G-TE performance, but the graphene film becomes less transparent, which in turn offsets the gains in G-TE performance. Figure 12 (c) shows the analysis of the dependence of R_{sh} on the work function WF, R_{sh} decreases upon a tiny shift of WF from its intrinsic value (4.66eV).Figure 12 (d) summarizes the R_{sh}–T curves of both the reported experimental data and our simulation results. The comparison between the original database and that obtained after training the ANN model indicates that the data obtained by the MLP are very close to the experimental values and our ANN model expresses faithfully the behaviour of the G-TE.
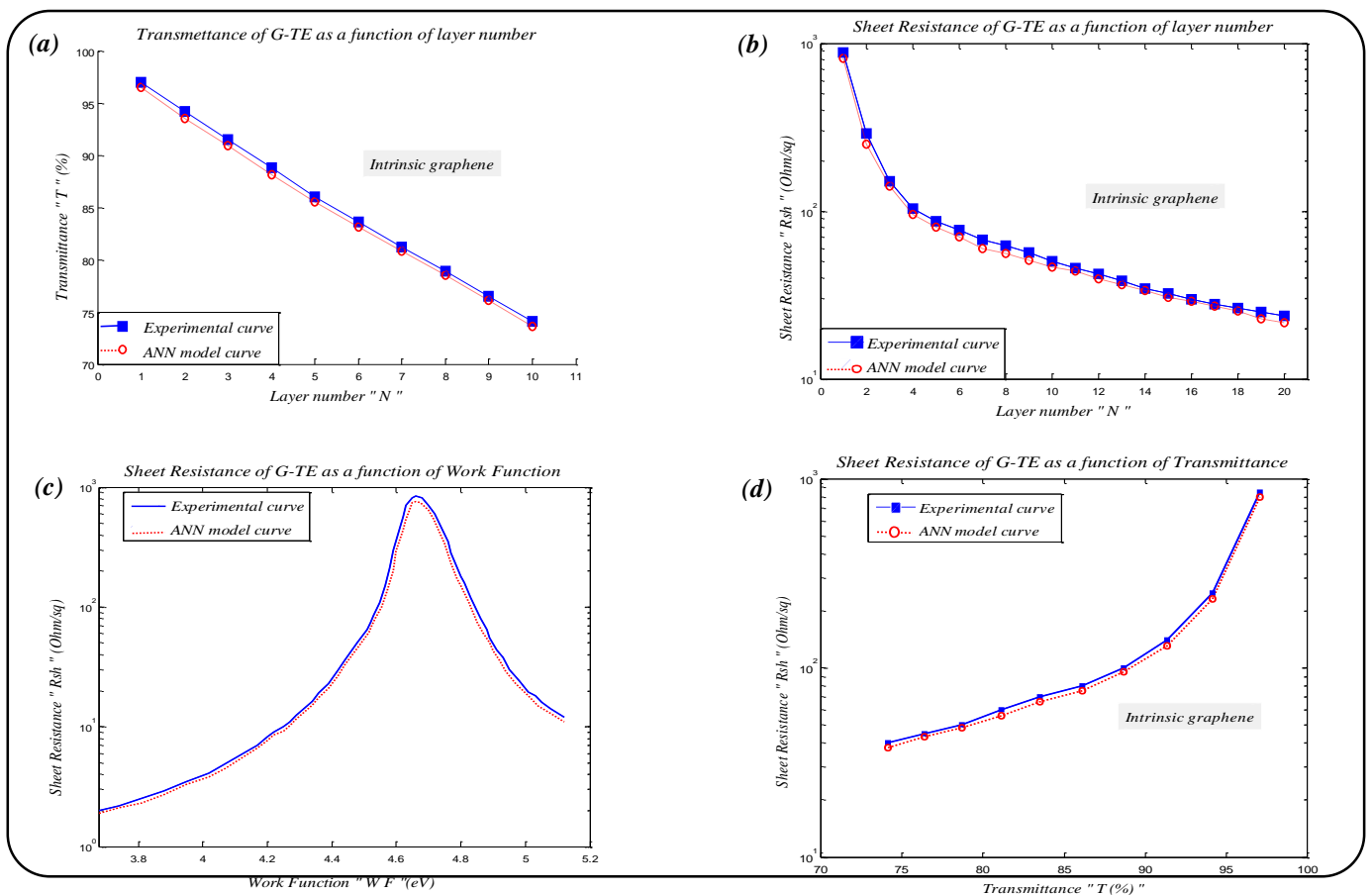

Fig. 11. ANN Model Performance for the different training curves

©2012-17 International Journal of Information Technology and Electrical Engineering

4.2. Prediction of G-TE Behaviour with the ANN Model

The performance of our ANN model is tested for inputs that have not been confronted by our system when training. In this phase the ANN model predict the behaviour of the G-TE with different input values.

Once the validity of the proposed method for G-TE behaviour has been verified, this methodology has been used to obtain different curves $R_{sh}(WF)$ for different N values as shown in figure 13(a) and $R_{sh}(T)$ for different WF values as shown in figure 13(b). Our calculations are presented in dashed lines. The solid lines plot the experimental data of graphene.

The engineering of work function WF and layernumber N of graphene plays an important role to affect the final device performance. As shown in figure 13 the proposed artificial neural networks provide an accurate prediction for the curves $R_{sh}(WF)$ for different N values and $R_{sh}(T)$ for different WF values of the G-TE. Our MLP was correctly trained; it tends to give reasonable responses. In table1, we selected input values who leads to output parameters close to I.T.O's performance.

We found that three layers of graphene with a work function of 4.75 eV leads to a sheet resistance of 50 Ω/sq and transmittance of 91.4 %.

Table 1
Input values leads to outputs close to I.T.O parameters

Input Parameters		Output Parameters	
N	WF (eV)	T(%)	R_{sh} (Ω/sq)
1	4.90	97.1	50
1	5.10	97.1	16
2	4.75	94.2	80
2	4.80	94.2	45
2	4.90	94.2	18
2	5.10	94.2	7
3	4.70	91.4	100
3	4.75	91.4	50
3	4.80	91.4	28
3	4.90	91.4	12
3	5.10	91.4	4
4	4.70	88.7	70
4	4.75	88.7	38
4	4.80	88.7	20
4	4.90	88.7	8
4	5.10	88.7	3

The present theoretical study is a clear demonstration of the useful combination of the properties of graphene as transparent conducting electrodes in Si solar cells, which provides high transmittance and good conductivity.
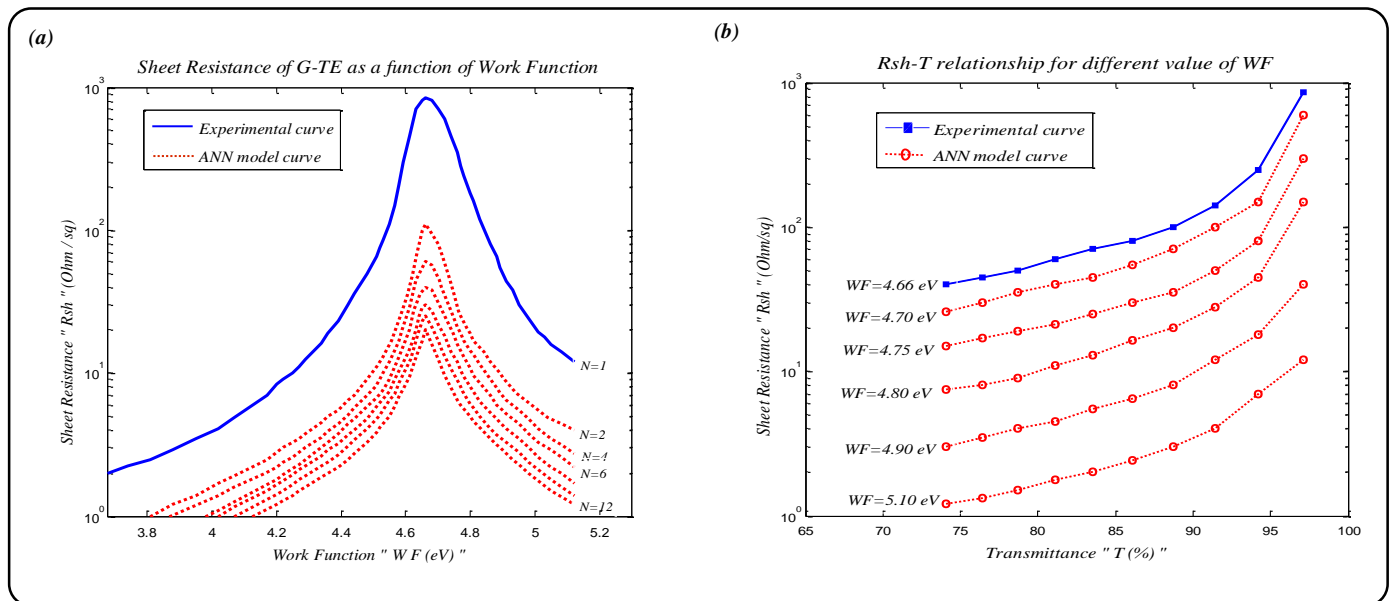

Fig. 12. ANN model prediction of G-TE behaviour.

5. CONCLUSION

The work presented in this article relates to the G-TE modelling with artificial neural networks, which is a very useful tool for PV system designers, because modelling could be applied before the G-TE fabrication, thus providing an appropriate behaviour of the G-TE incorporated in Si solar cells.

The graphene-based thin films were successfully applied as transparent electrodes working in Si Schottky solar cells. In comparison to similar solar cell devices using ITO as electrodes, graphene-based solar cells can deliver comparable photovoltaic performance. It is found that a good adjusting the two input parameters, which are, layer number and the work function of graphene reduce the sheet resistance and improve the transmittance, which in turn improve the G-TE solar cell performance. This work indicates that graphene-based electrodes have the potential to substitute ITO in a wide range of optoelectronic devices.

The ANN model requires a considerable database to ensure good training, it can be deduced that this model compromises simplicity, accuracy and flexibility in the choice of input and output variables, and it allowed us to define the values of WF and N necessary to obtain the transmittance and conductivity for our G-TE.

The present theoretical study gives a useful combination of the properties of graphene as transparent conducting electrodes in Si solar cells, which provides high electrical conductivity and high optical transparency. The theoretical predictions with the ANN model suggest that several recombination of input parameters are validated, however a compromise between this inputs and the G-TE production cost is an important point to study.

With the projected predictions, the G-TE can be expected to pass the industry requirement for the next generation of TCO, including application in solar cells.

REFERENCES

[1] S. Bae, H. Kim, Y. Lee, X. Xu, J. S. Park, Y. Zheng, J. Balakrishnan, T. Lei, H. R. Kim, Y. I. Song, Y. J. Kim, K. S. Kim, B. Ozyilmaz, J. H. Ahn, B. H. Hong and S. Iijima, "Roll-to-roll production of 30-inch graphene films for transparent electrodes," Nature nanotechnology, 5(8), 574–578, 2010

[2] C. Wadia, A. P. Alivisatos and D. M. Kammen, "Materials availability expands the opportunity for large-scale photovoltaic deployment," Environmental science & technology, 43(6), 2072–2077, 2009.

[3] K. Tvingstedt and O. Inganäs, "Electrode grids for ito-free organic photovoltaic devices," Advanced Materials, 19(19), 2893-, 2007.

[4] M. G. Kang, M. S. Kim, J. Kim and L. J. Guo, "Organic solar cells using nano in printed transparent metal electrodes," Adv. Materials, 20(23), 4408–4413, 2008.

[5] V. Bhosle, J. T. Prater, F. Yang, D. Burk, S. R. Forrest and J. Narayan, "Gallium-doped zinc oxide films as transparent electrodes for organic solar cell applications," J. Appl. Phys., 102(2), 023501-, 2007.

[6] F. Yang and S. R. Forrest, "Organic solar cells using transparent SnO_2 anodes," Advanced Materials, 18(15), 2018–2022, 2006.

[7] B. O'Connor, C. Haughn, K. H. An, K. P. Pipe and M. Shtein, "Transparent and conductive electrodes based on unpatterned, thin metal films," Appl. Phys. Lett., 93(22), 223304-, 2008.

[8] J. Meiss, M. K. Riede and K. Leo, "Towards efficient tin-doped indium oxide (ITO)-free inverted organic solar cells using metal cathodes," Appl. Phys. Lett., 94(1),013303-, 2009.

[9] K. S. Novoselov, A. K. Geim, S. V. Morozov, D. Jiang, Y. Zhang, S. V. Dubonos, I. V. Grigorieva and A. A. Firsov, "Electric field effect in atomically thin carbon films," Science, 306(5696), 666–669, 2004.

[10] C. Lee, X. Wei, J. W. Kysar and J. Hone, "Measurement of the elastic properties and intrinsic strength of monolayer graphene," Science, 321(5887), 385–388, 2008.

[11] R. R. Nair, P. Blake, A. N. Grigorenko, K. S. Novoselov, T. J. Booth, T. Stauber, N. M. R. Peres and A. K. Geim, "Fine structure constant defines visual transparency of graphene," Science, 320(5881), 1308-, 2008.

[12] K.V. Emtsev, A. Bostwick, K. Horn, J. Jobst, G. L. Kellogg, L. Ley, J. L. McChesney, T. Ohta, S. A. Reshanov, J. Röhrl, E. Rotenberg, A. K. Schmid, D. Waldmann, H. B. Weber and T. Seyller, "Towards wafer-size graphene layers by atmospheric pressure graphitization of silicon carbide……8(3), 203-207," Nat. Mater., 8(3), 203-207, 2009.

[13] C. Berger, Z. Song, X. Li, X. Wu, N. Brown, C. Naud, D. Mayou, T. Li, J. Hass, A. N. Marchenkov, E. H. Conrad, P. N. First and W. A. de Heer, "Electronic confinement and coherence in patterned epitaxial graphene," Science, 312(5777), 1191–1196,2006.

[14] S. Stankovich, D. A. Dikin, R. D. Piner, K. A. Kohlhaas, A. Kleinhammes, Y. Jia, Y. Wue, S. B. T. Nguyen and R. S. Ruoff, "Synthesis of graphene-based nanosheets via chemical reduction of exfoliated graphite oxide," Carbon, 45, 1558-, 2007.

[15] A. Reina, X. Jia, J. Ho, D. Nezich, H. Son, V. Bulovic, M. S. Dresselhaus and J. Kong, "Large area, few-layer graphene films on arbitrary substrates by chemical vapor deposition,"Nano letters, 9(1), 30–35, 2009.

[16] X. Li,W. Cai, J. An, S. Kim, J. Nah, D. Yang, R. D. Piner, A. Velamakanni, I. Jung, E. Tutuc, S. K. Banerjee, L. Colombo and R. S. Ruo, "Large-area synthesis of high-quality and uniform graphene films on copper foils," Science, 324(5932), 1312–1314, 2009.

[17] K. S. Kim, Y. Zhao, H. Jang, S. Y. Lee, J. M. Kim, J. H. Ahn, P. Kim, J. Y. Choi and B. H. Hong, "Large-scale pattern growth of graphene films for stretchable transparent electrodes," Nature, 457(7230), 706–710, 2009.

[18] F. Bonaccorso, Z. Sun, T. Hasan and A. C. Ferrari, "Graphene Photonics and Optoelectronics," .Nature Photon, 4, 611-622, 2010.

[19] M.Biron, "Croissance et transfert de graphène pour la fabrication d'électrodes transparentes," (Growth and transfert of G-TE). Univ. of Montreal, Canada, 2013.

[20] H. . Park, J. Meyer, S. Roth and V. Skákalová, "Growth and properties of few-layer graphene prepared by chemical vapor deposition," Carbon, 48(4), 1088–1094, 2010.

[21] X. Li, Y. Zhu, W. Cai, M. Borysiak, B. Han, D. Chen, R. D. Piner, L. Colombo and R. S. Ruo, "Transfer of large-area graphene films for high-performance transparent conductive electrodes," Nano letters, 9(12), 4359–4363, 2009.

[22] Q. Yu, L. A. Jauregui, W. Wu, R. Colby, J. Tian, Z. Su, H. Cao, Z. Liu, D. Pandey, D. Wei, T. F. Chung, P. Peng, N. P. Guisinger, E. A. Stach, J. Bao, S S. Pei and Y. P. Chen, "Control and characterization of individual grains and grain boundaries in graphene grown by chemical vapour deposition," Nature materials, 10(6), 443–449, 2011.

[23] J. Suk, W., A. Kitt, C. W. Magnuson, Y. Hao, S. Ahmed, J. An, A. K. Swan, B. B. Goldberg and R. S. Ruo, "Transfer of CVD-grown monolayer graphene onto arbitrary substrates," ACS nano, 5(9), 6916–6924, 2011.

[24] X. Liang, B. Sperling, I. Calizo, G. Cheng, C. A. Hacker, Q. Zhang, Y. Obeng, K. Yan, H. Peng, Q. Li, X. Zhu, H. Yuan, A. R. H. Walker, Z. Liu, L M. Peng and C. A. Richter, "Toward clean and crackless transfer of graphene," ACS nano, 5(11), 9144–9153, 2011.

[25] A. Guermoune, T. Chari, F. Popescu, S. S. Sabri, J. Guillemette, H. S. Skulason, T. Szkopek and M. Siaj, "Chemical vapor deposition synthesis of graphene on copper with methanol, ethanol, and propanol precursors," Carbon, 1–7, 2011.

[26] A. H. Castro Neto, F. Guinea, N. M. R. Peres, K. S. Novoselov andA. K. Geim, "The electronic properties of graphene," Rev. Mod. Phys., 81, 109–162 ; 2009.

[27] Y. Shi, K. K. Kim, A. Reina, M. Hofmann, L. J. Li and J. Kong, "Work function engineering of graphene electrode via chemical doping," ACS Nano, 4, 2689–2694, 2010.

[28] S. K. Behura, P. Mahala, A. Ray, I. Mukhopadhyay and O. Jani, "Theoretical simulation of photovoltaic response of graphene on semiconductors," Applied Physics-A, 111, 1159-1163, 2013.

[29] X. Miao,S. Tongay,M. K. Petterson, K. Berke, A. G. Rinzler, B. R. Appleton and A. F. Hebard, "High Efficiency Graphene Solar Cells by Chemical Doping," Nanoletters, 12, 2745-2750, 2012.

[30] B. S. Wu, Y. C. Lai, Y. H. Cheng, S. C. Yu, P. Yu and G. C. Chi,"Hybrid Multi-Layer Graphene/Si Schottky Junction Solar Cells," IEEE, 978, 2486-2489, 2013.

[31] Y. Ye and L. Dai, "Graphene-based Schottky junction solar cells," .Journal of Materials Chemistry, 22, 24224-24229, 2012.

[32] Y. C. Lai, B. S. Wu, S. C. Yu, P. Yu and G.C. Chi,"Doping of Monolayer Graphene for Silicon based Schottky Junction Solar Cells," IEEE, 978, 2436-2438, 2013.

[33] X. M. Li, H. W. Zhu, K. L. Wang, A. Y. Cao, J. Q. Wei, C. Y. Li, Y. Jia, Z. Li, X. Li, and D. H. Wu, "Graphene on silicon schottky junction solar cells," Adv. Mater., 22, 2743–2748, 2010.

[34] S. Ghosh, I. Calizo, D. Teweldebrhan, E. P. Pokatilov, D. L. Nika, A. A. Balandin, W. Bao, F. Miao and C. N. Lau, "Extremely high thermal conductivity of graphene," prospects for thermal management applications in nanoelectronic circuits, Appl. Phys. Lett., 92, 151911, 2008.

[35] H. K. Jeong, K. J. Kim, S. M. Kim and Y. H. Lee,"Modification of the electronic structure of graphene by viologen," Chem. Phys. Lett., 498, 168–171, 2010.

[36] Y. Yi, W. M. Choi, Y. H. Kim, J. W. Kim and S. J. Kang, "Effective work function lowering of multilayer graphene films by subnanometer thick AlOx overlayers," Appl. Phys. Lett, 98, 013505, 2011.

[37] Y. Lin, X. Li, D. Xie, T. Feng, Y. Chen, R. Song, H. Tian, T. Ren, M. Zhong, K. Wang and H. Zhu "Graphene/semiconductor heterojunction solar cells with modulated antireflection and

graphene work function," Energy &Environmental Science, 6, 108–115, 2013.

[38] C. Touzet, "Les réseaux de neurones artificielles" (Artificial Neural Networks), 1992.

[39] F. Junod and M. Bornoz, "A la découverte des réseaux de neurones" (Discovery of artificial neural networks), Yverdon, 2002.

[40] V.E. Sandana, D.J Rogers, F. Hosseini-Teherani, P. Bove and M. Razeghi,"Graphene versus Oxides for transparent electrode applications," Oxide-based Materials and Devices, 8626, 862603/1-9, 2013.

[41] R. G. Gordon, "Criteria for Choosing Transparent Conductors," .MRS Bull., 25(8), 52-57, 2000.

[42] F. Bonaccorso, A. Lombardo, T. Hasan, Z. Sun, L. Colombo and A. C. Ferrari, "Production and processing of graphene and 2d crystals," Materials Today, 15(12), 564-589, 2012.

[43] M. Parizeau,"Réseaux de neurones," (Neural networks), University of Laval, 2004.

[44] Z. Meziani,"Modélisation de modules Photovoltaïques," (Modellingphotovoltaic modules).University of Batna, Algeria, 2013.

[45] F. Sorin, L. Broussard and P. Roblin, "Régulation d'un processus industriel par réseaux de neurones," (Regulation of industrialprocess by neural networks) . Techniques de l'Ingénieur, traité Informatique industrielle, Doc : S 7 582.

[46] R. Kumar, B. R Mehta, M. Bhatnagar, S. Ravi, S. Mahapatra, S. Salkalachen and P. Jhawar, "Graphene as a transparent conducting and surface field layer in planar Si solar cells," Nanoscale Research Letters, 9, 349, 2014.

[47] P. Li , C. Chen, J. Zhang, S. Li , B. Sun and Q. Bao, "Graphene-based transparent electrodes for hybrid solar cells," Frontiers in materials, 1(26), 1-7, 2014.

[48] R. Tahar, "Application de l'intelligence artificielle au problème de la stabilité transitoire des réseaux électriques," (Application of Artificial Intelligence to the Problem of TransitionalStability of Electrical Networks), University of Constantine, Algeria, 2005.

[49] F. Trahi, "Prédiction de l'irradiation solaire globale pour la région de Tizi-Ouzou par les réseaux de neurones artificiels," (Prediction of global solar irradiation for the Tizi-ouzouregion by artificial neural networks), University of Tizi-Ouzou, Algeria, 2011.

[50] G. Foggia,"Pilotage optimal de système multi-sources pour le bâtiment," (Optimal control of multi-source system for thebuilding), University of Grenoble, France, 2009.

[51] K. Hornet, "Approximation capabilities of multilayer feedforward networks," Neural networks, 251-257, 1991.